13th Australasian Fluid Mechanics Conference
Monash University, Melbourne, Australia
13-18 December 1998

THE EFFECT OF AFTER-BODY GEOMETRY ON THE VORTEX-SHEDDING CHARACTERISTICS OF BLUFF BODIES

Nicole ROCKLIFF and Nathan STEGGEL

School of Mechanical and Materials Engineering
University of Surrey, Guildford, U.K.

ABSTRACT

The viscous flow around several different bluff body geometries (rectangles, triangles and T-shapes) of varying length-to-breath ratio L/D is investigated using a hybrid discrete vortex method. The results for the rectangular geometries show the drag coefficient increasing with decreasing length/breadth ratio, with no evidence of a maximum as observed experimentally at higher Reynolds numbers. The triangular geometries however show evidence of a maximum at $L/D \approx 0.2$. In both cases the Strouhal number St attains a maximum at about $L/D \approx 0.3$, but for relatively long bodies the shedding frequency appears to be much less for triangles than rectangles. The principle difference appears in the r.m.s. lift, with the lift forces on the triangles being much greater than for the rectangular bodies for all $L/D > 0.5$.

INTRODUCTION

The shedding of vortices by sharp-edged bluff bodies in incident flow has received a growing amount of attention in recent years. In particular there have been numerical studies at low to moderate Reynolds numbers by Davis and Moore (1982), Franke *et al* (1990), Nakayama *et al* (1993), Okajima *et al* (1993), Okajima (1995) and Sohankar *et al* (1997). Motivated by the use of various shaped bluffs in vortex flow meters, we examine the effects of a selection of body geometries including rectangles, triangles and T-shapes on the vortex-shedding characteristics. Ultimately we are interested in the effect of body geometry on "lock-in" between the frequency of a pulsating flow and the vortex shedding, which renders vortex flow meters unreliable. As it is first necessary to establish the shedding characteristics in a non-pulsating flow, here we examine the shedding behaviour of the various geometries in a two-dimensional uniform steady stream. In particular we examine the variation of drag, r.m.s. lift and Strouhal number (non-dimensional shedding frequency) with varying length/breadth ratio *L/D* and also, for similar *L/D,* the differences between the shapes.

The Reynolds number Re in all cases is set at 200, so that the flow is laminar. Experimental studies have also shown that this is the approximate threshold for the development of three-dimensional instabilities, so that our two-dimensional studies should be comparable with experimental results obtained at this Reynolds number. However such data currently exist only for rectangular cylinders and not the other geometries.

COMPUTATIONAL METHOD

The numerical method used in the study is a hybrid discrete vortex method, based on the work of Graham (1988). Such methods are particularly suitable for flows such as those under consideration, where there are regions of concentrated vorticity embedded within otherwise largely irrotational motion. Discrete vortex particles are introduced in the boundary layer and wake regions, and used to model the convection part of the vorticity transport; however the viscous diffusion of vorticity and the Poisson equation for the stream function are solved on a finite-difference grid.

In all cases, to simplify the calculations, the physical $z = (x, y)$ plane is mapped to a rectangular computational domain ($\Omega = (\xi, \eta)$) using a Schwarz-Christoffel type mapping for the exterior of a polygon to the exterior of a unit circle (see Bieberbach, 1953) and thence to the computational domain. The ξ axis, $0 \le \xi \le 2\pi$, represents the body surface and the outer boundary for the computations is set at η_{max}. The grid is regular in the ξ direction, but expands quadratically in the η direction.

The constraints associated with the mapping and its numerical implementation impose some restrictions on the geometries that can be modelled, particularly as the actual dimensions of the physical plane geometry are obtained as a result of the mapping. In the case of rectangular and triangular geometries, a single parameter (plus symmetry considerations) governs the overall shape, whilst with T-shapes there are three parameters, which govern the length/breadth ratio L/D and the relative thicknesses of stem and bar. However, for triangles and T-shapes, in order to be able to determine the physical dimensions exactly, it is necessary to choose the points corresponding to key vertices of the figure to be grid points in the computational plane; this then restricts, for example, the length/breadth ratios possible. As a consequence it is only possible to make comparisons between shapes with approximately the same ratio of B/A. It should also be noted that for T-shapes, it is not possible to prescribe all the vertex positions and so in fact the junction of stem and bar is frequently not a true sharp corner; this however does not appear to affect the results significantly.

In the general transformed co-ordinates of the computational plane, the velocities are defined as

$$\dot{\xi} = \frac{1}{J}\frac{\partial \psi}{\partial \eta}, \quad \dot{\eta} = -\frac{1}{J}\frac{\partial \psi}{\partial \xi},$$

and the vorticity as

$$\tilde{\omega} = \frac{1}{J}\left(\frac{\partial (J\dot{\eta})}{\partial \xi} - \frac{\partial (J\dot{\xi})}{\partial \eta}\right)$$

where ψ is the stream function. The Poisson equation relating the stream function to the vorticity becomes

$$\left(\frac{\partial^2}{\partial \xi^2} + \frac{\partial^2}{\partial \eta^2}\right)\psi = -J\tilde{\omega}.$$

The vorticity transport equation is split into two parts,

$$\left[\frac{\partial \tilde{\omega}}{\partial t}\right]_{diffusion} = \frac{\nu}{J}\nabla^2\tilde{\omega},$$

$$\left[\frac{\partial \tilde{\omega}}{\partial t}\right]_{convection} = \frac{\nu}{J}\nabla^2\tilde{\omega};$$

the first governs viscous diffusion, and is solved on the finite difference grid, whilst the second, convective part, is modelled by the advection of the point vortices. The time step of the calculations is in principle limited by the Jacobian of the transformation as well as by the smallest mesh size. The singularity in the Jacobian at the sharp corners is removed by a smoothing process using the values at adjoining mesh points, and the expansion of the mesh is controlled by the placing of the inner and outermost grid points. In this way adequate resolution of the boundary layer region can be maintained whilst allowing time steps large enough for the overall calculation time not to be prohibitive (even for low *L/D* where *J* becomes very small). (See Steggel,1998, for fuller details.)

The force coefficients are calculated at regular time intervals by integrating the spatial changes in pressure along mesh lines in the computational domain, (Steggel and Rockliff, 1997: Steggel, 1998). The dominant frequencies of the shedding process can then be extracted from these force-time histories.

UNIFORM FLOW RESULTS

Rectangles with body side ratios ranging between *L/D* = 0.02 and 4.0, triangles with *L/D* between 0.14 and 2.89, and two T-shapes, both with *L/D* = 1.0 but of different bar and stem thicknesses were considered.

For rectangular bodies in uniform flow the drag coefficient C_D was found to increase monotonically as *L/D* decreased (Figure 1) There was no evidence of the drag maximum observed at $L/D \approx 0.62$ in experimental studies at higher Reynolds numbers by Bearman and Trueman (1972), Laneville and Yong (1983) and others. However these results are consistent with the work of Sohankar *et al* (1997) who performed similar studies for $0.25 \le L/D \le 4.0$ using direct numerical simulation on a rectangular mesh, and with the other limited data available at Re = 200 principally for values of $L/D > 0.6$.

The Strouhal number however shows much more variation (Figure 2). Above $L/D = 1.0$ the numerical results give consistent values of $0.15 \le St \le 0.17$, and are typically about 10-20% higher than corresponding experimental results; this is thought to be due to the strictly two-dimensional nature of the numerical simulations whereas even in the best experimental set-ups three-dimensional effects can reduce the rate of vortex formation. Below $L/D = 1.0$ the Strouhal number first increases to a maximum near $L/D = 0.3$ and then decreases to close to its $L/D = 1.0$ value, as L/D decreases. These results are in good agreement with the direct numerical simulations of Sohankar *et al* (1997). Likewise the r.m.s. lift $C_{L(rms)}$ shows a maximum at close to $L/D = 0.3$.

For the isosceles triangle geometries the Strouhal number behaviour (Figure 3) is very close to that of the rectangular geometries for $L/D \le 1$; however, for larger length-to-breadth ratios, the Strouhal number for the triangular geometries appear to continue decreasing, unlike the gradual rise and levelling out of the rectangular body cases. The drag and r.m.s. lift coefficients for both geometry types are shown in Figures 4(a), (b). Whilst the triangular body drag exceeds that of the corresponding rectangular body at all times, the overall trend is similar, except that there is some evidence of a maximum in the drag at around $L/D = 0.2$.

The r.m.s. lift however is substantially larger for the triangles over much of the range, with the peak occurring at $L/D \approx 1.0$ as compared to the 0.3 value for rectangles. If the magnitude of the r.m.s. lift is taken as an indication of the strength of the vortex shedding process, then this indicates that triangular bluffs should be much more effective than rectangular ones. This is perhaps as expected.

One possible explanation lies in the fact that the separated region containing the vorticity remains in contact with the body for longer as it travels down the inclined side of the triangle, before the final shedding at the rear vertex. However, the explanation of Steggel (1998) for the peak in the r.m.s. lift at $L/D \approx 0.3$ for the rectangular body is capable of extension to the triangular shapes. The argument is as follows. Separation occurs at the front corner of the rectangle and a shear layer grows along the body. At the rear, the vortex shedding process dominates, resulting in oscillations of the shear layer, which in turn give rise to differences between the pressure distributions on top and bottom surface, and hence an oscillatory lift. Flow visualisations in the immediate vicinity of the body indicate that at low L/D the angle of inclination of the separating shear layers on either side can oscillate substantially during a shedding cycle, with a low surface pressure corresponding to the moment when the shear layer is closest to the surface. Near to the leading edge, as the shear layer is attached at the front vertex, this oscillation remains small, but further downstream, the shear layer has more freedom to oscillate. However, as the afterbody is extended, the trailing edge begins to interact with the separated layer,

damping out its oscillations. Thus the surface pressure can no longer oscillate so freely and the maximum magnitude of the lift begins to fall. In the case of the triangle, the geometry of the body means that the interaction of the trailing edge is delayed and also less, so that the peak in the lift occurs at higher L/D and the magnitude of the lift remains larger.

In addition to the two basic geometries above, we have also performed calculations for two T-shaped bodies, both with $L/D \approx 1.0$, but the first with relatively thin stem and bar ($D_2/D \approx 0.2$, $L_2/L \approx 0.2$) and the second with thick bar and stem ($D_2/D \approx 0.53$, $L_2/L \approx 0.57$). The results of these are shown are compared in Table 1 with the corresponding triangle and rectangle results. These are again consistent with the hypothesis of the effect of the trailing edge in reducing the ability of the shear layer to oscillate and hence generate large oscillations in the lift forces. The drag forces also appear to increase from the rectangular case, through thick and thin t shapes to the triangle. The variation on Strouhal number is less clear.

	St	C_D	$C_{L(rms)}$
rectangle	0.154	1.46	0.35
triangle	0.149	2.093	0.932
thin T	0.159	1.99	0.92
thick T	0.153	1.63	0.60

Table 1: Drag Coefficient and Strouhal number for the four different bodies with $L/D = 1.0$.

In the case of the thin T-shape it is interesting to regard this as a model of rectangle of length/breadth ratio 0.2 with an attached splitter plate and compare this with the 0.2 rectangle on its own. The corresponding results are: $St = 0.179$, $C_D = 2.42$, $C_{L(rms)} = 0.50$. The addition of a 'splitter plate' therefore seems to have the effect of increasing the lift, and decreasing the Strouhal number and the drag.

In Figure 5 we show a typical visualisation of the flow past a triangle. The separation from the trailing edge vertex is clearly shown; for this ratio of *L/D*, the vortex street remains strong and regular for some way downstream of the body.

CONCLUSION

The hybrid discrete vortex method can be used successfully to calculate low Reynolds number flows past various bluff geometries. It is found that the after-body geometry has a significant effect on the shedding characteristics. This is probably to the interaction (or lack of it) of the rear edge of the body with the separated shear layer which is formed on the body and which oscillates as a result of the shedding at the rear edge. With longer bodies and with ones with greater relative vertical dimension at the rear end, the presence of the body surface limits the oscillation and hence the possible lift force generated. This results in the triangular geometries, of the four shapes considered, at the same length/breadth ratio, generating the highest r.m.s. lift forces, which we believe to be a measure of the overall strength of the vortex shedding process. This suggests that triangular shapes therefore are likely to make the most effective bluffs for vortex flow meters.

REFERENCES

BEARMAN, P.W. and TRUEMAN, D..M. "An investigation of the flow around rectangular cylinders", *Aeronautical Quarterly* , 229-237, 1972.

BIEBERBACH, L. "*Conformal Mapping*" Chelsea Publishing Company, New York 1953.

DAVIS, R.W. and MOORE, E.F. "A numerical study of vortex shedding from rectangles" J. Fluid Mech. **116**, 475-506, 1982.

FRANKE, R., RODI, W., and SCHONUNG, B. "Numerical calculation of laminar vortex shedding flows past cylinders", *J. Wind Eng. & Indust. Aero.* **35**, 237-257, 1990.

GRAHAM, J.M.R "Computation of viscous separated flow using a particle method" , in *Numerical Methods in Fluid Mechanics* **3** , 310-317, (ed. K.W. Morton), Oxford University Press, Oxford, 1988.

LANEVILLE, A. and YONG,L.Z "Mean flow patterns around two-dimensional rectangular cylinders and their interpretation", *J. Wind Eng. & Indust. Aero.* **14**, 387-398, 1983.

NAKAYAMA, R., NAKAMURA, Y., OHYA, Y. and OZONO, S. "A numerical study on the flow around flat plates at low Reynolds numbers ", *J. Wind Eng. & Indust. Aero.*, **46-47**, 255-264, 1993.

OKAJIMA, A. KITAJIMA, K. and UENO, H "Numerical study on wake patterns and aerodynamic forces of an oscillating cylinder with a circular and rectangular cross-section.", *J. Wind Eng. & Indust. Aero.*, **50**, 255-264, 1993.

OKAJIMA, A. "Numerical analysis of the flow around an oscillating cylinder" in *Flow Induced Vibration* (ed. P. Bearman), Balkema, Rotterdam pp. 159-166, 1995.

SOHANKAR, A., NORBERG, C. and DAVIDSON, L., "Numerical Simulation of Unsteady Low-Reynolds Number Flow around Rectangular Cylinders at Incidence", *J. Wind Eng. & Indust. Aero.*, **69-71**, 189-201, 1997.

STEGGEL, N. , "A Numerical Investigation of the Flow Around Rectangular Cylinders", *Ph.D. Thesis*, University of Surrey, 1998.

STEGGEL,N. and ROCKLIFF, N. "Simulation of the effects of body shape on lock-in characteristics in pulsating flow by the discrete vortex method", *J. Wind Eng. & Indust. Aero.* **69-71**, 317-329, 1997.

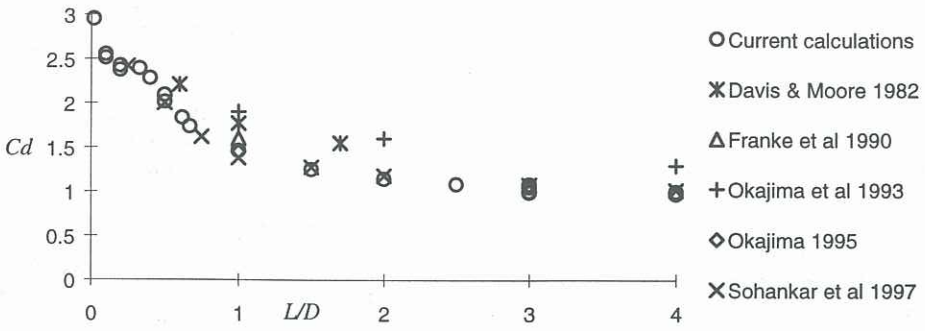

Figure 1 : Drag coefficient C_D vs. length/breadth ratio *L/D*, for rectangles , from various studies.

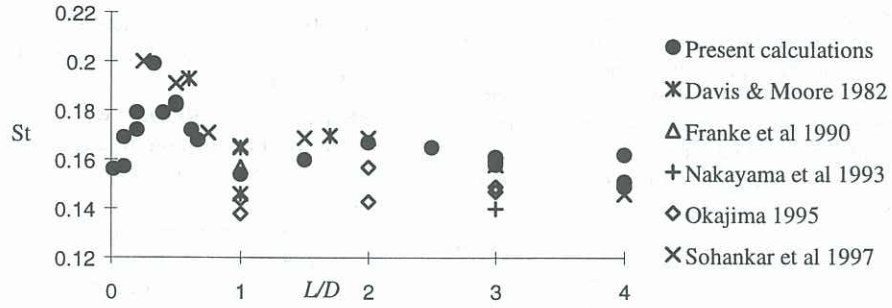

Figure 2: Strouhal number *St* vs. length/breadth *L/D,* for rectangles, from various studies.

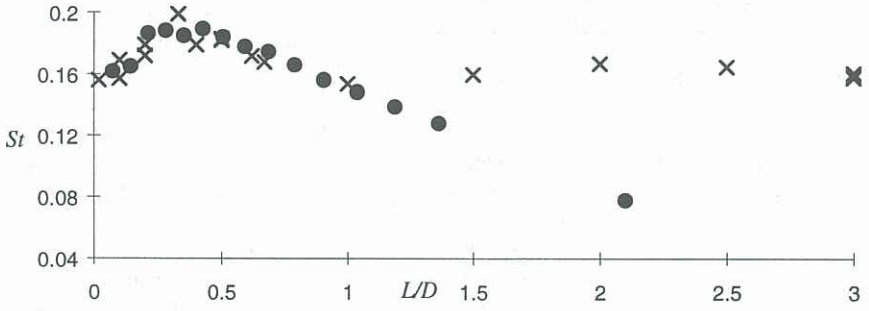

Figure 3 Strouhal number *St* vs. length/breadth ratio *L/D*; • triangles; × rectangles.

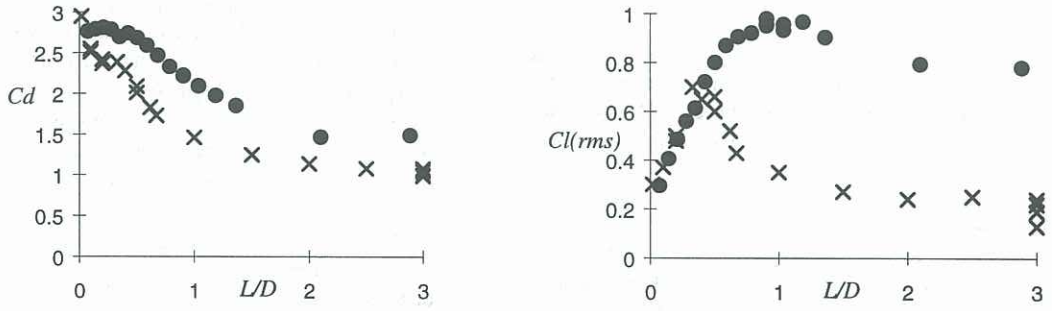

Figure 4 : Force coefficients C_D and $C_{L(rms)}$ for triangles (•) and rectangles(×).

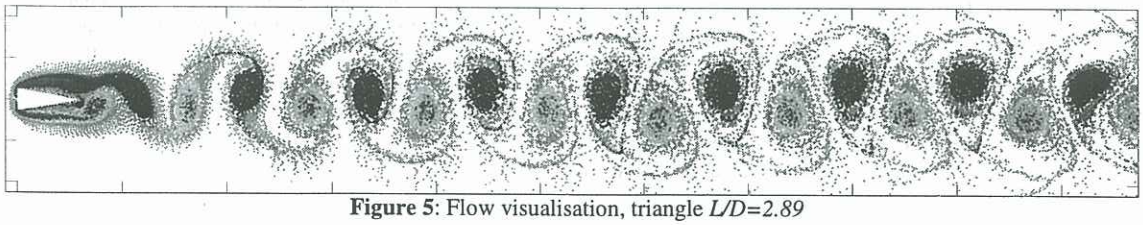

Figure 5: Flow visualisation, triangle *L/D=2.89*